



## Miniaturized electrochemical sensor for detection of mercury II ions

H. Nacer <sup>a,b\*</sup>, L. Bouzenada <sup>a</sup>, I. Hafaiedh <sup>c,d</sup>, R. Kherrat <sup>b</sup>, L. Hamlaoui <sup>b</sup>,  
R. Touzani <sup>e,f</sup>, N. Jaffrezic-Renault <sup>g</sup>

<sup>a</sup> Université de Tébessa, Route de Constantine, 12002 Tébessa Algérie

<sup>b</sup> Université Badji Mokhtar –Annaba, Laboratoire de Physicochimie des interfaces, BP12, El-Hadjar. Annaba 23000, Algérie.

<sup>c</sup> Nanotechnology Laboratory, INSAT, Centre Urbain Nord, 1080 Charguia Cedex, Tunisie.

<sup>d</sup> Unité de recherche de Physico-chimie des Matériaux Polymères, IPEST, 2070 La Marsa. Tunisia.

<sup>e</sup> LCAE-URAC18, COSTE, Faculté des Sciences, Université Mohammed Premier – BP 524, 60000 Oujda, Morocco.

<sup>f</sup> Faculté Pluridisciplinaire de Nador, BP300, Selouane 62700, Nador, Morocco.

<sup>g</sup> Université Claude Bernard. Lyon-1, Laboratoire des Sciences Analytiques, Bâtiment CPE. 43, Bd du 11 novembre 1918. 69622 Villeurbanne Cedex, France.

Received 13 Feb 2012, Revised 12 June 2012, Accepted 12 June 2012

\* Corresponding Author : Email: [nacerhouria@yahoo.fr](mailto:nacerhouria@yahoo.fr)

### Abstract

A PVC membrane electrode based on mercaptostyrenedivinylbenzene resin as the ionophore was prepared and was deposited on a platinum electrode. This one was characterized with impedance spectroscopy and modelled with an equivalent electric circuit. The detection of the mercury at low concentrations and the interaction with the other heavy metals were made by impedance measurements. The life expectancy of the membrane did not exceed one week.

**Keywords:** Impedance spectroscopy; mercaptostyrenedivinylbenzene resin; mercury (II) ions detection.

### 1. Introduction

Mercury detection devices are increasingly needed for health of the people working in industries, safety, environmental monitoring, and process control. To meet this demand, considerable research into new sensors is underway, including efforts to enhance the performance of traditional devices, such as resistive metal oxide sensors through nanoengineering. As an alternative, there has been great interest in trying to exploit the properties of organic materials [1-3]. As an alternative, there has been great interest to exploit organic molecular as ionophor for detection of mercury. In this work, we report a first attempt to use mercaptostyrenedivinylbenzene resin as the ionophore for exchanging ions in the detection of mercury in solution by electrochemicals impedance measurements.

#### 1.1. Mercury

Mercury is generally found at very low concentrations and is very reactive in the environment. It is a trace component of many minerals and economic ore deposits as native mercury and cinnabar. Because of its toxic nature and known ability to bio accumulate; low mercury loadings can pose a risk to receiving environments [4-7]. Mercury has also been considered as a human health hazard because it may cause kidney toxicity, neurological damage, paralysis, chromosome breakage, and birth defeats [8-10]. Elemental mercury is known to be responsible for causing damage to the sensory parts of the central nervous system. Toxicity of mercury

and the need for its determination in chemical analysis and environmental monitoring has generated increasing interest in the development of ion-selective electrodes for measurement of this analyte.

### 1.2. Electrochemical impedance spectroscopy

Electrochemical impedance spectroscopy (EIS) appears to be an excellent technique for the investigation of bulky and interfacial electrical properties of any kind of solid or liquid material connected to or being part of an appropriate electrochemical transducer [11-16]. It is a non-invasive technique that does not require complex or expensive instrumentation and is easy to operate, thus allowing its current applications not only in research laboratories but also as a tool for the control of processes such as the performance of batteries, semiconductors, or thin-film technology and by monitoring corrosion [17-20].

EIS has also been increasingly successful in the design and the development of sensor systems. We need to bear in mind the vast range of materials that may be used in their fabrication, as these may confer specific electric properties to the resulting device. Also, a great number of methodologies can be performed to integrate the appropriate recognition element with the transducer, which, in turn, gives rise to the generation of different interfaces with specific electric properties. In this context, the versatility of EIS allows its application to the control and monitoring of the different stages necessary for the fabrication of the sensor and its eventual characterisation. Also, EIS has been used successfully as a useful analytical tool for the development of sensor devices in a wide variety of configurations [22-30]. (EIS) appears to be an excellent technique for the measurement of electric property changes of the sensor system in the presence of increasing concentrations of the corresponding analyte. Based on the applications outlined above, the impedance analysis detection of Hg(II) ions using a PVC membrane based on mercaptostyrenedivinylbenzene resin as ionophore deposited on a platinum electrode, under controlled experimental conditions appears to be an excellent transduction protocol in the development of electrochemical sensor for mercury detection. The detection of Hg(II) ions in a PBS solution at very low concentrations, the interference with many heavy metals have been monitored by EIS and applied to the development of electrochemical sensor membrane for detection of mercury in waste water. We also studied this membrane by conductometric measurements and it shows a good selectivity for Hg(II) ions and the detections limits for conductometric measurements were  $10^{-7}$  mM. Electric impedance spectroscopy is a sensitive technique, which monitors the electrical response of the system studied after application of a periodic small amplitude ac signal. Analysis of the system response provides information concerning the electrical behaviour of the interface and interaction occurring on it [31, 32].

### 1.3. The resin

The ionophore used is a mercaptostyrenedivinylbenzene copolymer which has mainly functional thiol groups and a number of sulfonic groups and exhibits a macroporous structure [33]. The -SH groups are characterized by very low acidity degree ( $pK_a \approx 10,8$ ), their redox potential is +135 mV. Due to the presence of -SH groups, strong affinity of this cation exchanger for Hg (II) ions enables reactions of Hg (II) ions with mercaptans, thiolphenols, or hydrogen sulphide. Its capacity from Hg (II) ions is 240g Hg/dm<sup>3</sup> of ion exchanger. For comparison: using reduction methods, it is possible to diminish the mercury content in wastewaters down 1-3 ppm by precipitation of HgS, with hydrogen sulphide to 1ppm and applying the ion exchanger Imac-TMR to 0,5 – 6,0 ppb [34]. Despite of the fact that in the concentrated brines, Hg(II) occurs mainly in the form of the complex ions  $[HgCl_4]^{2-}$  Imac-TMR reacts mainly with  $Hg^{2+}$  and  $HgCl^+$  ions which are in the equilibrium in the solution [35].

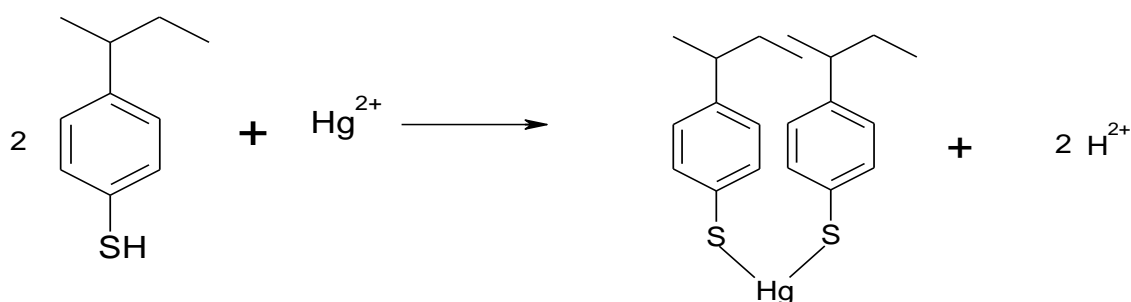
#### Equation 1:



Hg (II) ions sorption the ion exchange Imac-TMR can be described by means of the following reactions:

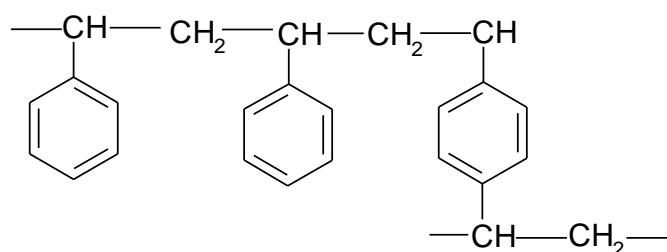
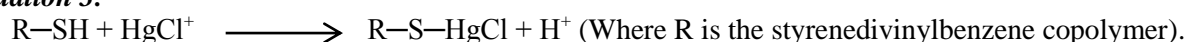
#### Equation 2:





**Scheme1.** Hg (II) ions sorption by the imac-TMR resin

**Equation 3:**



**Scheme 2.** The mercaptostyrenedivinylbenzene copolymer

After the Hg (II) ions sorption, the ion exchange Imac-TMR can be regenerated by means of the concentrated hydrochloric acid solution. Its unique thiol functionality makes this resin an interesting building block for the functionalities and can be used for the selective removal of other metals.

**2. Experimental:**

**2.1. Materials**

Mercaptostyrenedivinylbenzene resin was obtained from Rohm and Haas Company. Di-isononyl, tetrahydrofuran and high molecular weight polyvinylchloride (PVC) were purchased from Sigma-Aldrich chemie GmbH (Stein, Germany). All other reagents were pure analytical grade and were used without any further treatment.

**2.2. Preparation of the membrane:**

The mixture composition used to obtain the membrane was 10 mg of the ground resin (grain diameter around 1 μm), 33 mg PVC and 67 mg of plasticizer (diisononyl phthalate) were added to 1ml of THF and deposited on the sensitive area of the working platinum electrode.

The membrane is then dried in the nitrogen during approximately 30 minutes before use.

**3. Results and discussions:**

Before use, the platinum electrode was cleaned with acetone bath for 10 min and dried under nitrogen flow, followed by immersion in a Pirhana solution (7:3 v/v, H<sub>2</sub>SO<sub>4</sub>:H<sub>2</sub>O<sub>2</sub>) for 1 min in order to get rid of inorganic and organic contaminants on the substrate surface. They were subsequently rinsed thoroughly in absolute ultra pure water and finally dried under nitrogen flow.

**3.1. Characterization of the platinum electrode with cyclic voltammetry technique**

Cyclic voltammetry of an electroactive species such as K<sub>4</sub>[Fe(CN)<sub>6</sub>] /K<sub>3</sub>[Fe(CN)<sub>6</sub>]<sub>4</sub> is a valuable tool for testing the kinetic barrier of an interface. The extent of kinetic limitation of the electron transfer process

increases with the increasing thickness and decreasing defect density of the barrier. Therefore, it was decided to investigate changes in electrode behaviour after the deposit of the membrane, using these electroactive species. When an electrode surface has been modified by some materials, the electron transfer kinetics is perturbed. **Fig. 1** shows cyclic voltammograms obtained on the naked platinum in a PBS solution (curve "a") and after the deposit of the membrane on the platinum electrode in a solution containing the redox couple  $K_4[Fe(CN)_6]/K_3[Fe(CN)_6]$  at a 5 mM concentration (curve "c") and the membrane deposited on platinum in a PBS solution (curve "b").

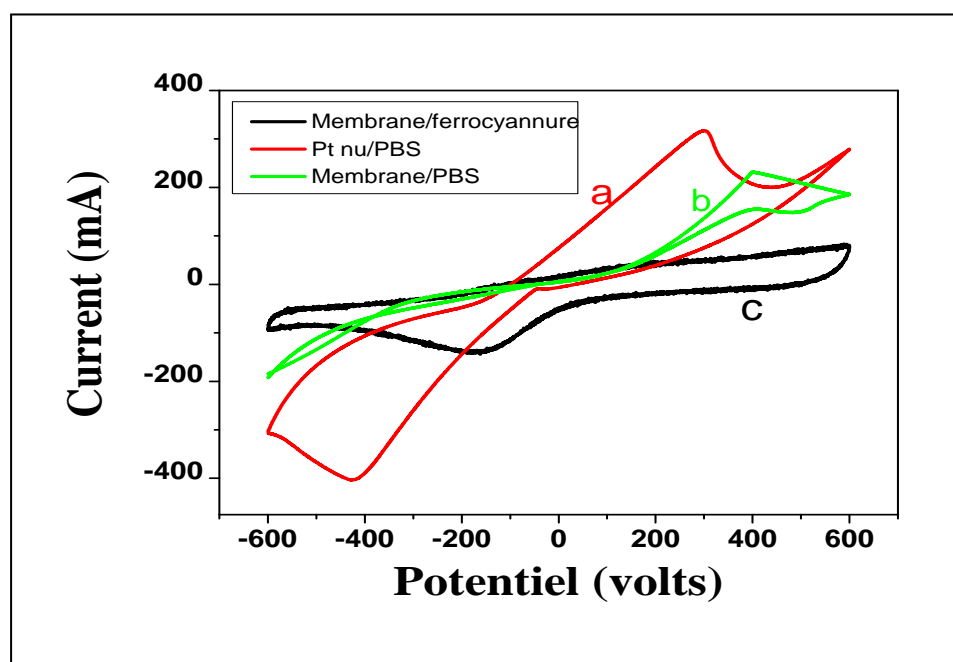


**Figure 1:** Cyclic voltammetric measurements

Membrane – Pt electrode in PBS solution (curve "b") and in a 5 mM redox probe of the couple  $K_3[Fe(CN)_6]/K_4[Fe(CN)_6]$  (curve "c"): and of the naked platinum electrode in a PBS solution (curve "a"). All experiments were performed at Potential rate = -600 mV/s, potential step = 100 mV, step duration = 20 seconds, initial frequency = 100 kHz, final frequency = 100 mHz and Amplitude = 10 mV.

Cyclic voltammetry experiments can confirm that the membrane layer was successfully formed on the platinum surface when the electrode surface was modified by the deposit of the membrane, the electron transfer kinetics of the redox couple  $K_4[Fe(CN)_6]/K_3[Fe(CN)_6]$  were perturbed. The curve "a" shows a reversible process of the redox reaction to the surface of the platinum. After the deposit of the membrane, the peaks of the redox process decrease, what shows that the deposited layer decreases the faradic process of the working electrode in the redox solution of couple  $K_4[Fe(CN)_6]/K_3[Fe(CN)_6]$  (curve "c"), and in the PBS solution (curve "b").

### 3.3. Impedance analysis of the membrane based on mercaptostyrene-divinylbenzene:

We notice on the **Fig. 2**, two buckles of impedance variation corresponding to the coupling interfacial capacity - charge-transfer resistance  $R_{tc}$  (in the compulsory potential  $E_0 = -200$  mV) characterized by the frequency  $f_c = 100$  mV: the first buckle is the "capacitive buckle", it allows in principle the values of charge-transfer resistance  $R_{tc}$  (determination of the beam of the circle arc), of  $C_d$  (from the values of diffusional capacity  $C_d$  and  $R_{tc}$ ) and of the resistance of cell  $R_c$  (by extrapolation of the circle's arc up to the axis of the realities, at infinite frequency (**Fig. 3**)). A second buckle at low-frequency corresponding to the dominant intervention of the process faradique (transfer of load) in the interface of the electrode and the diffusional process).

The passage of alternating current by the process interfacial capacitif being then blocked) (it is however still about an effect of type capacitif, the angle  $\phi$  is positive. This buckle which we indicate by the term of " buckle of diffusion " can be characterized by the frequency  $f_d$ , its amplitude measured on the axis of the realities is a function at the same time of  $R_{tc}$  and of characteristics of the involved diffusionnel process, in particular of the thickness of the diffusionnel layer . Both characteristic frequencies  $f_c$  and  $f_d$  play an important role as far as, of their values depends the effective observation on the experimental diagram of these two separate buckles or at least a part enough very unobservable by being situated in the field of frequency above the experimental limit high frequency HF. In contrast, the same thing occurs for the diffusionnel buckle if  $f_d$  is too low being situated above the experimental limit low frequency LF.

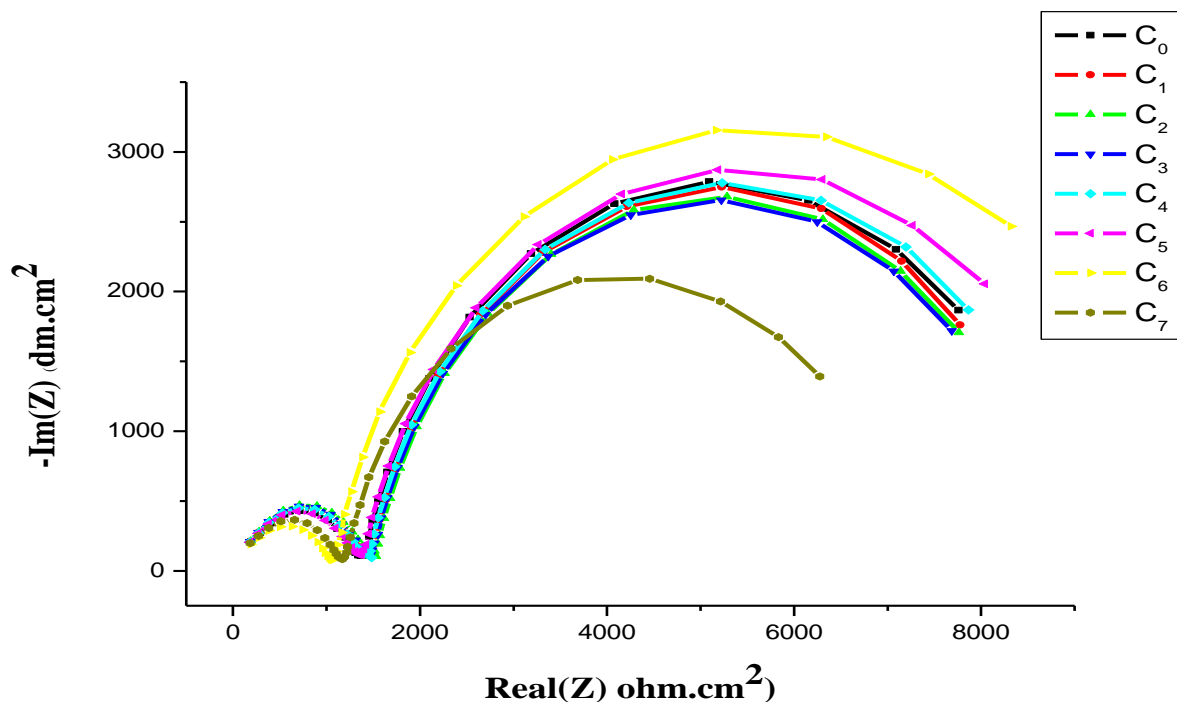


**Figure 2:** Nyquist diagram (Real (Z) vs. -Im (Z)) for the impedance measurements corresponding to the detection of mercury ions II.

All measurements were performed in a PBS solution pH 6,5. Potential rate = - 200Mv, potential step = 0 mV, step duration = 20second, initial frequency = 100 kHz, final frequency = 100 mHz and Amplitude = 10 mV.  $C_0$ :PBS solution;  $C_1=3,98 \cdot 10^{-6}$  M;  $C_2=3,96 \cdot 10^{-6}$  M;  $C_3= 3,94 \cdot 10^{-6}$  M;  $C_4=3,9210^{-6}$  M;  $C_5=3,90 \cdot 10^{-6}$  M;  $C_6=3,88 \cdot 10^{-6}$  M;  $C_7=3,86 \cdot 10^{-6}$  M

In summary, we have two half circles; the diameter of half a circle at low frequency being all the bigger as the electrochemical system is fast more the value of  $R_{tc}$  is low. Half a circle at LF can be likened to the formation of a not conductive movie on the surface of electrode, we could assimilate this movie, from the point of view of the electric equivalence with a resistance ( $R_3$  it serie with a warburg element pair of shorts  $W_s$  (warburg short), which is Equivalent to the impedance of warburg  $Z_w$  connected to the broadcasting, quite there parallele with a CPE (constant phase element), the set(group) is mass with the electrochemical interface (the Resistance  $R_2$  ( $R_{tc}$ ) in series with a Ge (Gerisher element), these two last ones assembly being in parallel with a capacity  $C_1$  as the electric model indicates (Fig.7) realized by modelling on the software ZView.

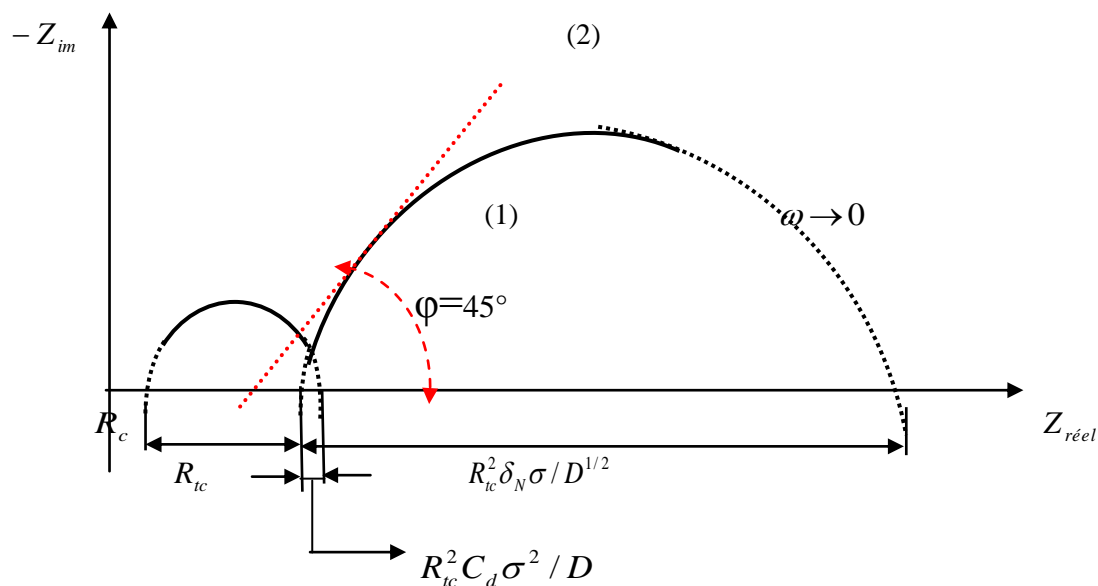


**Figure 3:** Representation in the complex plan of a capacitive buckle + diffusionnel buckle (case of a complete thickness diffusion).

### 3.4. Modelling on the software ZView

The diagrams of impedance (**Fig. 2**) are treated by means of the software ZView (Scribner Associate, Inc) who allows the construction of equivalent electric circuits and the adjustment of spectres by means of these circuits. Every buckle of the curve was analyzed to part. For the first buckle capacitive, the software gave the consisted circuit the resistance of the solution R1, the resistance of charge transfer R2 and the capacity C1. The model of curve given by the software with these three elements is not stacked in the capacitive buckle obtained experimentally (**Fig. 4**) with a coefficient of correlation equal to 0,02 %.

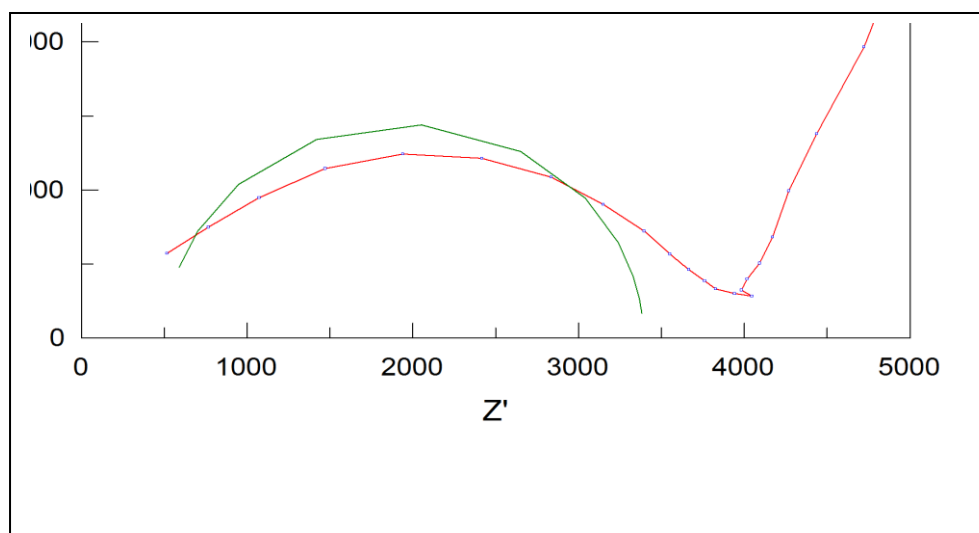


**Figure 4:** Simplistic illustration of modelling of the capacitive buckle with Resistance / capacity circuit

The addition of the Gerisher element for the same buckle, improves considerably the modelling and we observe an overlapping of both curves (**Fig. 5**), the experimental one and the one proposed by the model with an error on the various parameters of the order of 0,002 %.

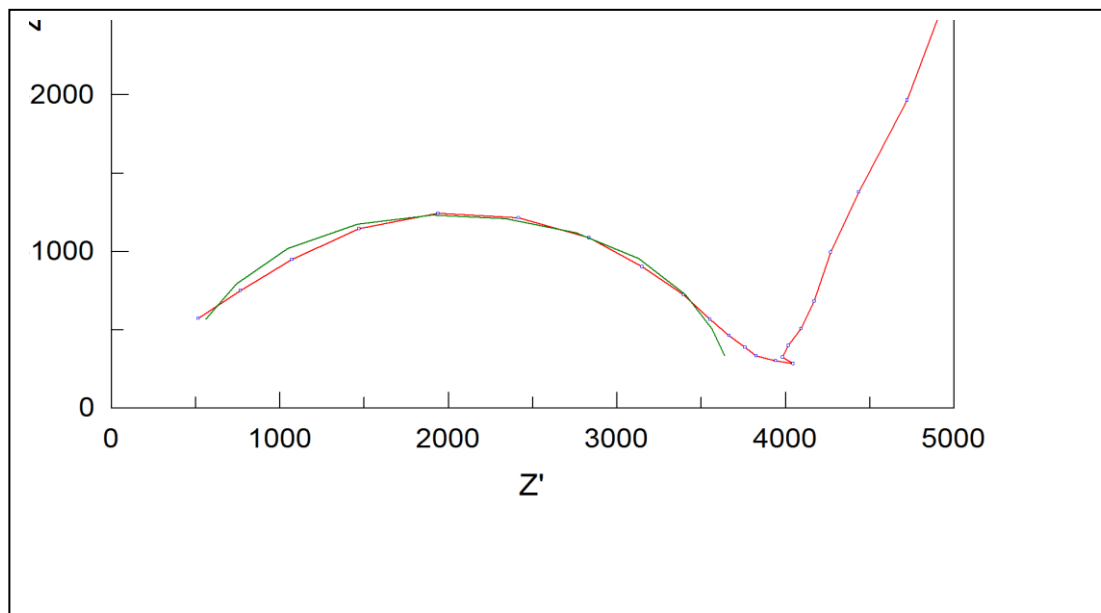


**Figure 5:** Simplistic illustration of the capacitive buckle modelling with the circuit R/C + Ge (Gerisher element).

The electric model will thus be for the first buckle High frequency of the following shape:

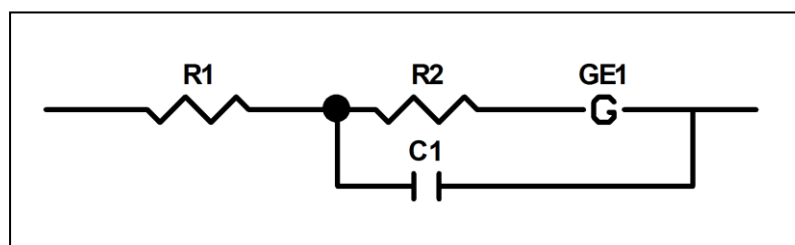


**Figure 6:** Electric circuit for half - encircles HF

**Table 3.1 :** Parameters stemming from the fittage with the circuit of **Fig. 6** of Nyquist Diagrams with various concentrations of  $Hg^{2+}$ .

Pot	Concentration	Rs	Rtc	C(F)	GE1-T	GE-1P	$\chi^2$
-200mV	PBS without addition	146,9	661,5	6,787E-9	1,2717E-5	25893	0,002
	$C_1= 3,98 \cdot 10^{-6} \text{ M}$	141,8	652,6	6,703E-9	1,0397E-5	30670	0,001
	$C_2=3,96 \cdot 10^{-6} \text{ M}$	136,6	642,8	6,614E-9	9,3372E-6	34727	0,001
	$C_3= 3,94 \cdot 10^{-6} \text{ M}$	134,3	638,3	6,716E-9	9,639E-6	35130	0,001
	$C_4=3,9210^{-6} \text{ M}$	132,4	626,6	6,729E-9	9,9763E-6	34850	0,001
	$C_5=3,90 \cdot 10^{-6} \text{ M}$	130,8	595,6	6,783E-9	1,0231E-5	40456	0,001
	$C_6=3,88 \cdot 10^{-6} \text{ M}$	140,6	569,8	7,753E-9	2,7823E-5	13282	0,008
	$C_7=3,86 \cdot 10^{-6} \text{ M}$	129,6	549,5	6,917E-9	1,2711E-5	38140	0,001

The electric model for the whole curve is illustrated on the **Fig. 8** knowing that the capacitive buckle gave the parameters stemming from the fitting and collected in the Table 3.1. As you can see The **Fig. 7** shows an overlapping of both curves; that experimental and that stemming from the electric model what justifies the sensible choice of elements constituting the electric circuit.

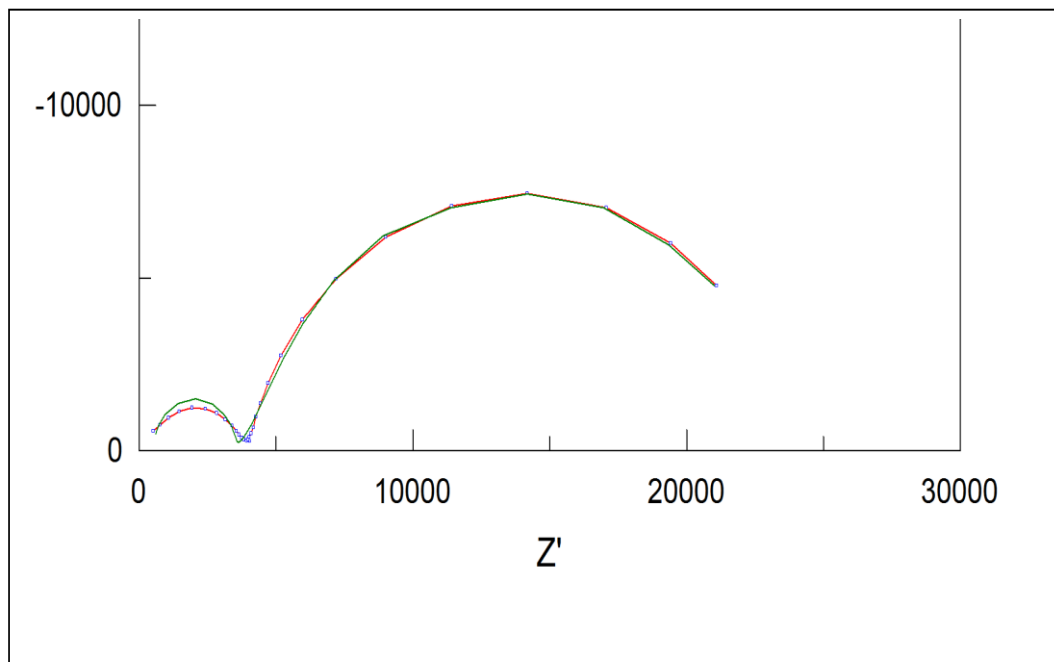


**Figure 7 :** Overlapping of both curves; experimental and that stemming from the electric model of the software ZVIEW.

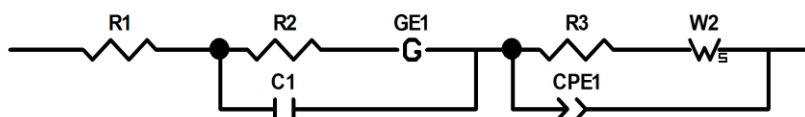


**Figure 8:** Electric model of the Nyquist diagrams with various concentrations of  $Hg^{2+}$

The results presented in the (Table 3.1) show those charge-transfer resistance increases with the increase of the concentration of the  $Hg^{2+}$  ions. To draw the curve of calibration, we represented the variation of the charge-transfer resistance  $\Delta R_{tc}$  (Table 3.2) according to the concentration of the mercury in PBS solution (**Fig. 9**) and we notice that  $\Delta R_{tc}$  is proportional in the concentration of the mercury injected in the solution.

**Table 3.2:** Variation of the transfer charge resistance according to the concentration of mercury ions

Concentration	$\Delta R = R_{tc} \text{ (PBS solution)} - R_{tc}$
0	$661.5 - 661.5 = 0$
$3.98 \cdot 10^{-6}$	$661.5 - 652.6 = 8.9$
$3.96 \cdot 10^{-6}$	$661.5 - 642.8 = 18.7$
$3.94 \cdot 10^{-6}$	$661.5 - 638.3 = 23.2$
$3.92 \cdot 10^{-6}$	$661.5 - 626.6 = 34.9$
$3.90 \cdot 10^{-6}$	$661.5 - 595.6 = 65.9$
$3.88 \cdot 10^{-6}$	$661,5 - 569,8 = 91,7$
$3,86 \cdot 10^{-6}$	$661,5 - 549,5 = 112$



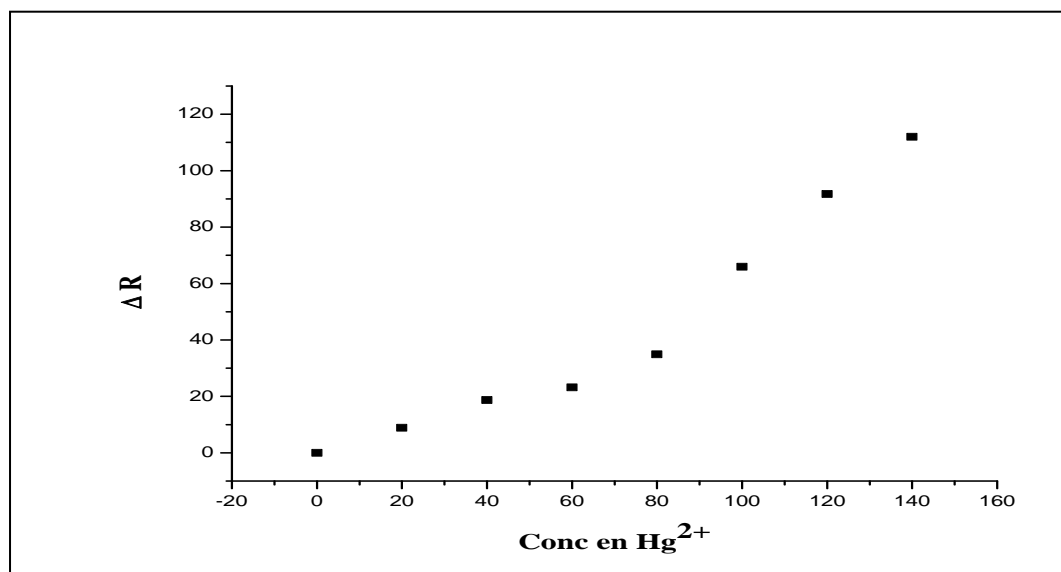


**Figure 9:** Calibration curve

### 3.5. Life duration of the membrane:

We have tested the membrane for a week, the **Fig. 10** indicated that the membrane works well for six day and the seventh day we didn't have any response.

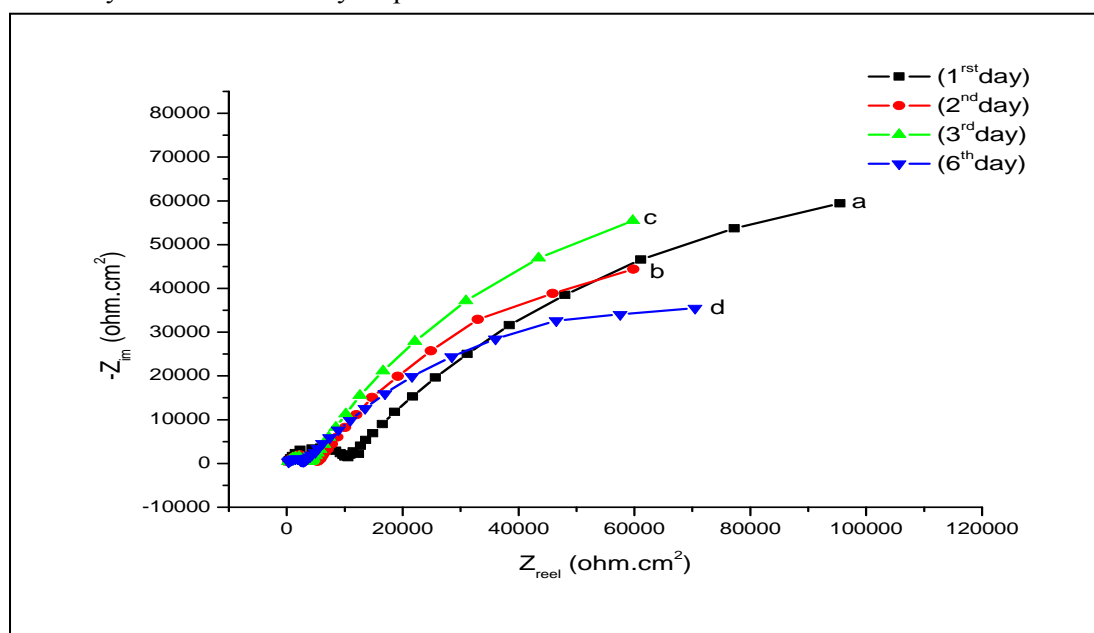


**Figure 10:** Life duration of the sensor.

All measurements were performed in a PBS solution pH 6,5. Potential rate = - 200Mv, potential step = 0 mV, step duration = 20second, initial frequency = 100 kHz, final frequency = 100 mHz, Amplitude = 10mV

## Conclusion

In this paper, we studied the analysis of PVC membrane electrode based on mercaptostyrenedivinylbenzene resin as the ionophore, by impedance spectroscopy in the presence of low concentrations of mercury ions II and we found that the resistance of charge transfer (R<sub>tc</sub>) increases with the concentration of mercury in the PBS solution. The electric circuit editing the electrochemical cell is obtained by modelling the impedance diagrams using the software Zview, then we tested during a week the smooth running of the sensor and we found that the membrane is effective during almost one week.

## References

1. R. Touzani, S. El Kadiri, A. Zerrouki, S. Scorrano, G. Vasapollo, M.G. Manera, R. Rella, Lecture Notes in Electrical Engineering 91 (2011) 81.
2. R. Touzani, G. Vasapollo, S. Scorrano, R. Del Sole, M.G. Manera, R. Rella, S. El Kadiri, Materials Chemistry and Physics 126 (2011) 375.
3. R. Touzani, S. El Kadiri, A. Zerrouki, S. Scorrano, G. Vasapollo, M.G. Manera, F. Casino, R. Rella, Arabian Journal of Chemistry, 2012, under press.
4. T. Suzuki, R.A. Goyer, M.A. Mehlman (Eds.), Toxicology of Trace Elements, Hemisphere, Washington DC, 1977.
5. S.P. Bhaysar, E. Awad, C.G. Mahon, S. Petro, Ecotoxicology, 20 (2011) 1588.
6. S.A. Mansour, NATO Science for Peace and Security Series A: Chemistry and Biology, (2011) 73.
7. S. Ando, K. Koide, Journal of The American Chemical Society, 133 (2011) 2556.
8. L. Magos, in: I. Gut, M. Cikrt, G.L. Plaa (Eds.), Industrial and Environmental Xenobiotics, Springer-Verlag, Berlin, 1981, p. 1.
9. Y. Zhang, D. Gao, V.J. Bolivar, D.A. Lawrence, Toxicological Sciences, 119 (2011) 270.
10. J. Mutter, A. Curth, J. Naumann, R. Deth, H. Walach, Journal of Alzheimer's Disease, 22 (2010) 357.
11. A.J. Bard, L.R. Faulkner, Electrochemical Methods: Fundamental and Applications, Wiley, New York, USA, 1980.
12. R. Wang, J. Di, J. Ma, Z. Ma, Electrochimica Acta, 61 (2012) 179.
13. L. Wang, J. Zhao, X. He, J. Gao, J. Li, C. Wan, C. Jiang, Intern. J. Electrochem. Sci. 7 (2012) 345.
14. A.H. Ismail, C. Schäfer, A. Heiss, M. Walter, W. Jahmen-Dechent, S. Leonhardt, Biosensors and Bioelectronics 26 (2011) 4702.
15. J. Segalini, B. Daffos, P.L. Taberna, Y. Gogotsi, P. Simon, Electrochimica Acta, 55 (2010) 7489.
16. B.-Y. Chang, S.-M. Park, Annual Review of Analytical Chemistry 3 (2010) 207.
17. J.R. McDonald, Impedance Spectroscopy: Emphasizing Solid Materials and Systems, Wiley, New York, USA, 1987.
18. C.R. Magana-Zavala, M.E. Angles-San Martin, F.J. Rodriguez-Gomez, D.R. Acosta, R. Avila-Godoy, B. Hidalgo-Prada, Anti-Corrosion Methods and Materials 57 (2010) 118.
19. A.P. Borole, D. Aaron, C.Y. Hamilton, C. Tsouris, Environ. Sci. Technol. 44 (2010) 2740.
20. Z. He, F. Mansfeld, Energy and Environmental Science, 2 (2009) 215.
21. X. Cui, D. Jiang, P. Diao, J. Li, R. Tong, X. Wang, Electroanal. Chem. 470 (1999) 9.
22. C. Fernandez-Sanchez, C. J. McNeil, K. Rawson, TrAC-Trends in Analytical Chemistry, 24 (2005) 37.
23. A. Jossen, Encyclopedia of Electrochemical Power Sources, (2009) 478.
24. R.A. Gerhardt, Encyclopedia of Condensed Matter Physics, (2005) 350.
25. J.L. Gilbert, Comprehensive Biomaterials, 1(2011) 21.
26. B. piro, J. Haccoun, M.C. Pham, L.D. Tran, A. Rubin, H. Perrot, C. Gabrielli, Journal of Electroanalytical Chemistry 577 (2005) 155.
27. A.T.A. Jenkins, R.D. Armstrong, Journal of Applied Electrochemistry, 25 (1995) 1143.
28. A. Amirudin, D. Thiény, Progress in Organic Coatings, 26 (1995) 1.
29. F. Mansfeld, Journal of Applied Electrochemistry 25 (1995) 187.
30. M. Palencia, B.L. Rivas, E. Pereira, A. Arrieta, Polymer Bulletin, 65 (2010) 145.
31. X. Cui, D. Jiang, P. Diao, J. Li, R. Tong, X. Wang, Electroanal. Chem. 470 (1999) 9.
32. I. Navratilova, P. Skladal, Bioelectrochemistry 62 (2004) 11.
33. G.J. De Jong, G.J.N. Reckers, J. Chromatogr. 102 (1974) 443.
34. Akzo Zout Chemie, The Akzo Imac TMR process for the removal of mercury from waste water. Akzo Zout Chemie, Hengelo 1975.
35. R. Bogoczek, E. Kociolek-Balawejder, kogut, A, Usowanie jonów w, rtoci zesciekow. Praem. Chem. 68 (1989) 83.

(2012) ; <http://www.jmaterenvironsci.com>